

# Inclusive semileptonic fits, heavy quark masses, and $V_{cb}$

Paolo Gambino

*Dip. di Fisica, Univ. di Torino, & INFN Torino, I-10125 Torino, Italy*

and

Christoph Schwanda

*Institut für Hochenergiephysik, Wien, Austria*

## Abstract

We perform global fits to the moments of semileptonic  $B$  decay distributions and extract  $|V_{cb}|$ , the heavy quark masses, and the non-perturbative parameters of the heavy quark expansion. We include NNLO perturbative corrections and recent determinations of the charm mass, and discuss how they improve the precision of the global fit. In particular, using the  $m_c$  determination of Ref. [11] we get  $m_b^{kin} = 4.541(23)$  GeV and  $|V_{cb}| = (42.42 \pm 0.86) \times 10^{-3}$ . We also discuss the implications of the new fits for the normalization of rare  $B$  decays, the zero-recoil sum rule in  $B \rightarrow D^* \ell \nu$ , and the inclusive determination of  $|V_{ub}|$ .

# 1 Introduction

The CKM matrix elements  $V_{cb}$  and  $V_{ub}$  are important ingredients in the analyses of CP violation in the Standard Model and in the search for new physics in flavor violating processes. For instance, the absolute value of their ratio gives one of the sides of the unitarity triangle, and the  $\varepsilon_K$  constraint on  $\bar{\rho}$  and  $\bar{\eta}$  is very sensitive to the precise value of  $|V_{cb}|$ , see [1] for recent analyses. The determination of  $V_{cb}$  and  $V_{ub}$  from inclusive semileptonic  $B$  decays is based on an Operator Product Expansion (OPE) that allows us to express the widths and the first moments of the kinematic distributions of  $B \rightarrow X_{u,c}\ell\nu$  as double expansions in  $\alpha_s$  and  $\Lambda_{QCD}/m_b$ . The leading terms in these double expansions are given by the free  $b$  quark decay, and the first corrections are  $O(\alpha_s)$  and  $O(\Lambda_{QCD}^2/m_b^2)$  [2].

The relevant parameters of the double expansions are the heavy quark masses  $m_b$  and  $m_c$ , the strong coupling  $\alpha_s$ , and the  $B$ -meson matrix elements of local operators of growing dimension:  $\mu_\pi^2$  and  $\mu_G^2$  at  $O(1/m_b^2)$ ,  $\rho_D^3$  and  $\rho_{LS}^3$  at  $O(1/m_b^3)$ , etc. The latter can be constrained by various moments of the lepton energy and hadron mass distributions of  $B \rightarrow X_c\ell\nu$  that have been measured with good accuracy at the  $B$ -factories, as well as at CLEO, DELPHI, CDF. The total semileptonic width can then be employed to extract  $|V_{cb}|$ . The situation is less favorable in the case of  $|V_{ub}|$ , where the total rate is much more difficult to access, but the results of the semileptonic fits are crucial in that case as well, see [3] for a review. This strategy has been rather successful and has allowed for a  $\sim 2\%$  determination of  $V_{cb}$  and for a  $\sim 5\%$  determination of  $V_{ub}$  from inclusive decays [4].

Complementary studies of exclusive decays and non-perturbative calculations of the relevant form-factors have also progressed considerably, reaching a similar level of accuracy. Unfortunately, a  $\sim 2\sigma$  discrepancy persists between the most precise determinations of  $|V_{cb}|$ : the inclusive one and the one based on  $B \rightarrow D^*\ell\nu$  at zero recoil and a lattice calculation of the form-factor [4, 5]. However, the zero-recoil form-factor estimate based on heavy quark sum rules leads to  $|V_{cb}|$  in good agreement with the inclusive result [6]. A stronger discrepancy between the inclusive and exclusive determinations occurs in the case of  $|V_{ub}|$  [4].

The importance of a precise and reliable extraction of  $|V_{cb}|$  and of the inputs for the inclusive  $|V_{ub}|$  analysis has motivated us to critically re-examine the procedure used in the semileptonic fits almost a decade after the first comprehensive studies [7–9]. There are three relevant issues in this respect: *i*) the theoretical uncertainties and how they are implemented in the fit, *ii*) the inclusion of additional constraints on the parameters, *iii*) the need to update the theoretical predictions to NNLO.

For what concerns the theoretical uncertainties, we have already observed [10] a marked dependence of the results on the ansatz for the correlations among theoretical uncertainties at different values of the cut on the lepton energy. In this paper we discuss different options and compare the results of the fits performed accordingly.

Regarding the inclusion of additional constraints from other processes, we recall that the semileptonic moments are sensitive to a linear combination of  $m_c$  and  $m_b$ , but cannot resolve the individual masses with good accuracy. To improve the accuracy of the fit, the moments of the photon energy in  $B \rightarrow X_s\gamma$  have generally been employed, but in the last few years quite precise determinations of the heavy quark masses by completely different methods ( $e^+e^-$

sum rules, lattice QCD etc.) have become available, see *e.g.* [11–15]. Radiative moments remain very interesting, but they are not competitive with the charm mass determinations and are in principle subject to additional  $O(\Lambda_{QCD}/m_b)$  effects, which have not yet been estimated [16]. Here we will discuss the inclusion of the most recent heavy quark mass determinations in the semileptonic fit. As we will see, these precise external inputs reduce the dependence on the assumptions regarding the theoretical correlations.

Recent progress has made it necessary to update the theoretical predictions used in the fits. The NNLO  $O(\alpha_s^2)$  calculation has been completed [17–19] and implemented [20] in a code that has been used in preliminary analyses by the Heavy Flavor Averaging Group [4]. This code extends and improves on the kinetic scheme calculation of Ref. [21], used in [7, 9], and forms the basis of the present work. The NNLO accuracy is a necessary prerequisite for using the precise heavy quark mass constraints we have just mentioned. Concerning the perturbative corrections to the Wilson coefficients of power-suppressed operators, the  $O(\alpha_s \mu_\pi^2/m_b^2)$  have been computed in [22, 23]. However, the  $O(\alpha_s \mu_G^2/m_b^2)$  corrections are not yet available and here we will not include any  $O(\alpha_s/m_b^2)$  corrections. Concerning higher order power corrections, the  $O(1/m_b^4)$  and  $O(1/m_Q^5)$  effects have been computed [24]. The main problem here is a proliferation of non-perturbative parameters that cannot all be fitted from experiment. In Ref. [24] they were estimated in the ground state saturation approximation, leading to a final  $O(1/m_Q^{4,5})$  effect on  $|V_{cb}|$  of +0.4%. This may well be the order of magnitude of higher order power corrections, but further investigations are necessary, also because sizable effects beyond the ground state saturation approximation have been found [6]. Here, we include only effects up to  $O(1/m_b^3)$  [25].

The paper is organized in the following way. We first discuss the relevant observables and list all the moment measurements included in our fits. Then, in Section 3, we explain our estimate of theoretical errors and discuss several options for their correlations. In Section 4 we consider the inclusion of independent constraints on  $m_c$  and  $m_b$  in the fits and study their impact on the results; then, in Section 5, we consider a few relevant applications of the fits. Finally, Section 6 contains a summary of our results.

## 2 Observables included in the fits

The first few moments of the charged lepton energy spectrum in inclusive  $b \rightarrow c \ell \nu$  decays are experimentally measured with high precision — better than 0.2% in the case of the first moment. At the  $B$ -factories a lower cut on the lepton energy,  $E_\ell \geq E_{cut}$ , is applied to suppress the background. Experiments measure the moments at different values of  $E_{cut}$ , which provides additional information as the cut dependence is also a function of the OPE parameters. The relevant quantities are therefore

$$\langle E_\ell^n \rangle_{E_\ell > E_{cut}} = \frac{\int_{E_{cut}}^{E_{max}} dE_\ell E_\ell^n \frac{d\Gamma}{dE_\ell}}{\int_{E_{cut}}^{E_{max}} dE_\ell \frac{d\Gamma}{dE_\ell}}, \quad (1)$$

	experiment	values of $E_{cut}$ (GeV)	Ref.
$R^*$	BaBar	0.6, 1.2, 1.5	[26, 27]
$\ell_1$	BaBar	0.6, 0.8, 1, 1.2, 1.5	[26, 27]
$\ell_2$	BaBar	0.6, 1, 1.5	[26, 27]
$\ell_3$	BaBar	0.8, 1.2	[26, 27]
$h_1$	BaBar	0.9, 1.1, 1.3, 1.5	[26]
$h_2$	BaBar	0.8, 1, 1.2, 1.4	[26]
$h_3$	BaBar	0.9, 1.3	[26]
$R^*$	Belle	0.6, 1.4	[28]
$\ell_1$	Belle	1, 1.4	[28]
$\ell_2$	Belle	0.6, 1.4	[28]
$\ell_3$	Belle	0.8, 1.2	[28]
$h_1$	Belle	0.7, 1.1, 1.3, 1.5	[29]
$h_2$	Belle	0.7, 0.9, 1.3	[29]
$h_{1,2}$	CDF	0.7	[31]
$h_{1,2}$	CLEO	1, 1.5	[32]
$\ell_{1,2,3}$	DELPHI	0	[33]
$h_{1,2,3}$	DELPHI	0	[33]

Table 1: Experimental data used in the fits unless otherwise specified.

which are measured for  $n$  up to 4, as well as the ratio  $R^*$  between the rate with and without a cut

$$R^*(E_{cut}) = \frac{\int_{E_{cut}}^{E_{max}} dE_\ell \frac{d\Gamma}{dE_\ell}}{\int_0^{E_{max}} dE_\ell \frac{d\Gamma}{dE_\ell}}. \quad (2)$$

This quantity is needed to relate the actual measurement of the rate with a cut to the total rate, from which one conventionally extracts  $|V_{cb}|$ . Since the physical information that can be extracted from the first three linear moments is highly correlated, it is more convenient to study the central moments, namely the variance and asymmetry of the lepton energy distribution. In the following we will consider only  $R^*$  and

$$\ell_1(E_{cut}) = \langle E_\ell \rangle_{E_\ell > E_{cut}}, \quad \ell_{2,3}(E_{cut}) = \langle (E_\ell - \langle E_\ell \rangle)^{2,3} \rangle_{E_\ell > E_{cut}}. \quad (3)$$

Similarly, in the case of the moments of the hadronic invariant mass distribution, we consider

$$h_1(E_{cut}) = \langle M_X^2 \rangle_{E_\ell > E_{cut}}, \quad h_{2,3}(E_{cut}) = \langle (M_X^2 - \langle M_X^2 \rangle)^{2,3} \rangle_{E_\ell > E_{cut}}. \quad (4)$$

These observables can be expressed as double expansions in  $\alpha_s$  and inverse powers of  $m_b$ , schematically

$$M_i = M_i^{(0)} + \frac{\alpha_s(\mu)}{\pi} M_i^{(1)} + \left(\frac{\alpha_s}{\pi}\right)^2 M_i^{(2)} + M_i^{(\pi)} \frac{\mu_\pi^2}{m_b^2} + M_i^{(G)} \frac{\mu_G^2}{m_b^2} + M_i^{(D)} \frac{\rho_D^3}{m_b^3} + M_i^{(LS)} \frac{\rho_{LS}^3}{m_b^3} + \dots \quad (5)$$

where all the coefficients  $M_i^{(j)}$  depend on  $m_c$ ,  $m_b$ ,  $E_{cut}$ , and on various renormalization scales. The OPE parameters  $\mu_\pi^2$ , ... are matrix elements of local  $b$ -fields operators evaluated in the physical  $B$  meson, *i.e.* without taking the infinite mass limit. The dots represent missing terms of  $O(\alpha_s/m_b^2)$  and  $O(1/m_b^4)$ , which are either unknown or we do not include for the reasons explained in the Introduction. We work in the kinetic scheme [34] and follow the implementation described in [20, 21]. In particular, in the hadronic moments we do not expand in powers of  $\bar{\Lambda} = M_B - m_b$ . While we always express the bottom mass and the four relevant expectation values that appear in Eq. (5) in the kinetic scheme setting the cutoff  $\mu^{kin}$  at 1 GeV, we will use both the kinetic and the  $\overline{\text{MS}}$  scheme for the charm mass, and denote it with  $m_c^{kin}(\mu^{kin})$  and  $\overline{m}_c(\bar{\mu})$ , respectively. Unless otherwise specified we evaluate  $\alpha_s$  at  $\mu_0 = 4.6$  GeV and assume  $\alpha_s(\mu_0) = 0.22$ . A change of  $\pm 0.005$  around this value leads to small changes in the results of our fits (about 1 MeV in  $m_b$ ), always much smaller than their final uncertainty.

The experimental data for the moments are fitted to the theoretical expressions in order to gain information on the non-perturbative parameters and the heavy quark masses, which we then employ to extract  $|V_{cb}|$ . Table 1 shows the 50 measurements of the moments which we always include in the fits, unless otherwise specified. The chromomagnetic expectation value  $\mu_G^2$  is also constrained by the hyperfine splitting

$$M_{B^*} - M_B = \frac{2}{3} \frac{\mu_G^2}{m_b} + O\left(\frac{\alpha_s \mu_G^2}{m_b}, \frac{1}{m_b^2}\right).$$

Unfortunately, little is known of the power corrections to the above relation and only a loose bound can be set, see [6] for a recent discussion. For what concerns  $\rho_{LS}^3$ , it is somewhat constrained by the heavy quark sum rules. Following [6, 21, 35], we will therefore use in our fits the constraints

$$\mu_G^2 = (0.35 \pm 0.07) \text{ GeV}^2, \quad \rho_{LS}^3 = (-0.15 \pm 0.10) \text{ GeV}^3. \quad (6)$$

It should be stressed that  $\rho_{LS}^3$  plays a minor role in the fits because its coefficients are generally suppressed with respect to the other parameters.

We now perform a first global fit, without any theoretical uncertainty. The fit is not good, with  $\chi^2/dof \sim 2$ , corresponding to a very small  $p$ -value and driven by a strong tension ( $\sim 3.5\sigma$ ) between the constraints in Eq. 6 and the measured moments. If we drop the constraints of Eq. 6 the fit is not too bad. It is then clear from the outset that theoretical uncertainties are not so much necessary for the OPE expressions to fit the moments — that would merely test Eq.(5) as a parameterization; they are instead needed to preserve the definition of the parameters as  $B$  expectation values of certain local operators, which in turn can be employed in the semileptonic widths and in other applications of the Heavy Quark Expansion.

### 3 Theoretical errors and their correlations

The OPE description of semileptonic moments is subject to two sources of theoretical uncertainty: missing higher order terms in Eq. (5) and terms that violate quark-hadron duality,

namely terms that are intrinsically beyond the OPE. We will attempt an estimate only of the first kind of uncertainty. The violation of local quark-hadron duality is expected to be suppressed in semileptonic  $B$  decays; it would manifest itself as an inconsistency of the fit, which as we will see is certainly not present at the current level of theoretical and experimental accuracy.

To estimate the effects due to higher order corrections we follow the method outlined in [21] and update it with the suggestions given in [20]: we assume that perturbative corrections can affect the Wilson coefficients of  $\mu_\pi^2$  and  $\mu_G^2$  at the level of  $\pm 20\%$ , while perturbative corrections and higher power corrections can effectively change the coefficients of  $\rho_D^3$  and  $\rho_{LS}^3$  by  $\pm 30\%$ . Moreover we assign an irreducible theoretical uncertainty of 10 MeV to the heavy quark masses, and vary  $\alpha_s(m_b)$  by 0.02. The changes in  $M_i$  due these variations of the fundamental parameters are added in quadrature and provide a theoretical uncertainty<sup>1</sup>  $\delta M_i^{th}$ , to be subsequently added in quadrature with the experimental one,  $\delta M_i^{exp}$ . This method is consistent with the residual scale dependence observed at NNLO, and appears to be reliable: the NNLO corrections and the  $O(1/m_b^{4,5})$  (using ground state saturation as in [24]) have been found to be within the range of expectations based on the method in the original formulation of [21].

The correlation between theoretical errors assigned to different observables are much harder to estimate, but they play an important role in the semileptonic fits, as it will become clear in a moment. Let us first consider moments computed at a fixed value of  $E_{cut}$ : as long as one deals with central higher moments, there is no argument of principle supporting a correlation between two different moments, for instance  $\ell_1$  and  $h_2$ . We also do not observe any clear pattern in the known corrections, and therefore regard the theoretical predictions for different central moments as completely uncorrelated. When one computes the theory uncertainty with the method described above, one might think there are obvious correlations: suppose that both  $\ell_1$  and  $h_2$  receive *positive* contributions from  $\mu_\pi^2$ ; by varying  $\mu_\pi^2$  by  $\pm 20\%$  we see a *positive* correlation between  $\ell_1$  and  $h_2$ . But our aim was simply to have a rough estimate of the *size* of the theory uncertainty, and we make no claim to know the *exact magnitude* and *sign* of the higher-order correction! Therefore, the observed correlation is meaningless and the safest assumption is to regard the theoretical predictions for different moments as uncorrelated.

Let us now consider the calculation of a certain moment  $M_i$  for two close values of  $E_{cut}$ , say 1 GeV and 1.1 GeV. Clearly, the OPE expansion for  $M_i(1 \text{ GeV})$  will be very similar to the one for  $M_i(1.1 \text{ GeV})$ , and we confidently expect this to be true at any order in  $\alpha_s$  and  $1/m_b$ . The theoretical uncertainties we assign to  $M_i(1 \text{ GeV})$  and  $M_i(1.1 \text{ GeV})$  will therefore be very close to each other and *very highly correlated*. The degree of correlation between the theory uncertainty of  $M_i(E_1)$  and  $M_i(E_2)$  can intuitively be expected to decrease as  $|E_1 - E_2|$  grows. Moreover, we know that higher power corrections are going to modify significantly the spectrum only close to the endpoint. Indeed, one observes that the  $O(1/m_b^{4,5})$  contributions are equal for all cuts below about 1.2 GeV (see Fig.2 of [24]) and the same happens for

---

<sup>1</sup>This theoretical uncertainty depends of course on the exact point in the parameter space. In practice we adopt an iterative procedure recomputing the theory errors on the minimum  $\chi^2$  point till the process has converged.

the  $O(\alpha_s \mu_\pi^2 / m_b^2)$  corrections [22]. Therefore, the dominant sources of current theoretical uncertainty suggest very high correlations among the theoretical predictions of the moments for cuts below roughly 1.2 GeV.

In Refs. [7, 9], it has been assumed that the theoretical errors of moments at different values of  $E_{cut}$  are 100% correlated. This is too strong an assumption, which ends up distorting the fit, because the dependence of  $M_i$  on  $E_{cut}$ , itself a function of the fit parameters, is then free of theoretical uncertainty. As a result, the uncertainty on the OPE parameters is underestimated. On the other hand, as we have just discussed, a high degree of correlation is to be expected if  $E_{cut}$  is not too large. Ref. [8] sets the theoretical correlation matrix equal to the experimental one. This probably underestimates correlations, and also implies no correlation between the theoretical prediction of the *same* observable measured by two independent experiments, which is patently absurd.

An alternative approach consists in computing the correlation of the theoretical errors of  $M_i(E_1)$  and  $M_i(E_2)$  using the method we have used to estimate the theory uncertainty, namely varying the values of the HQE parameters. This is in fact equivalent to assuming that the  $E_{cut}$ -dependence of the unknown terms of the OPE follows closely the  $E_{cut}$ -dependence of the known terms. It turns out that in this way the correlation is almost always very high.

Another possibility is to fix the correlation  $\xi$  between a moment  $M_i$  computed at  $E_{cut}$  and at  $E_{cut} + 0.1$  GeV, possibly with  $\xi$  higher for higher  $E_{cut}$ . Following the reasoning above,  $\xi$  is naturally very close to 1 at low cuts, and drops considerably at high cuts.

In our fits, we will consider the following four options:

- A** 100% correlation between moments at different cuts;
- B** correlations computed from theory predictions, as discussed above;
- C** constant scale factor  $0 < \xi < 1$ , with  $\xi = 0.97$  for 100 MeV steps;
- D** a scale factor like in **C** that depends on the cut,  $\xi = \xi(E_{cut})$ , with

$$\xi(E_{cut}) = 1 - \frac{1}{2} e^{-\frac{(E_0 - E_{cut})}{\Delta}} \quad (7)$$

where  $E_0 \approx 1.75$  GeV is the partonic endpoint and  $\Delta$  is an adjustable parameter which we set at about 0.25 GeV.

As an illustration, the correlation between the theoretical errors of a generic moment with cuts at 0.6 and 1.2 GeV is 1 in scenario **A**; it depends on the specific moment and it is generally quite close to 1 in scenario **B**; it is given by  $\xi^6 = (0.97)^6 \simeq 0.83$  in scenario **C**; it is given by  $\prod_{k=0}^{k=5} \xi(0.65 + 0.1k \text{ GeV}) \simeq 0.88$  in scenario **D**. Similarly, the correlation between a moment measured at 1.3 and 1.5 GeV is approximately 0.94 in **C** and 0.76 in **D**.

In Fig. 1 we show the results of semileptonic fits performed with the four options for the theoretical correlations. The fits include all the data listed in Table 1 and the two constraints of Eq. (6). We add the experimental and theoretical covariance matrices, which is equivalent to adding the respective errors in quadrature.

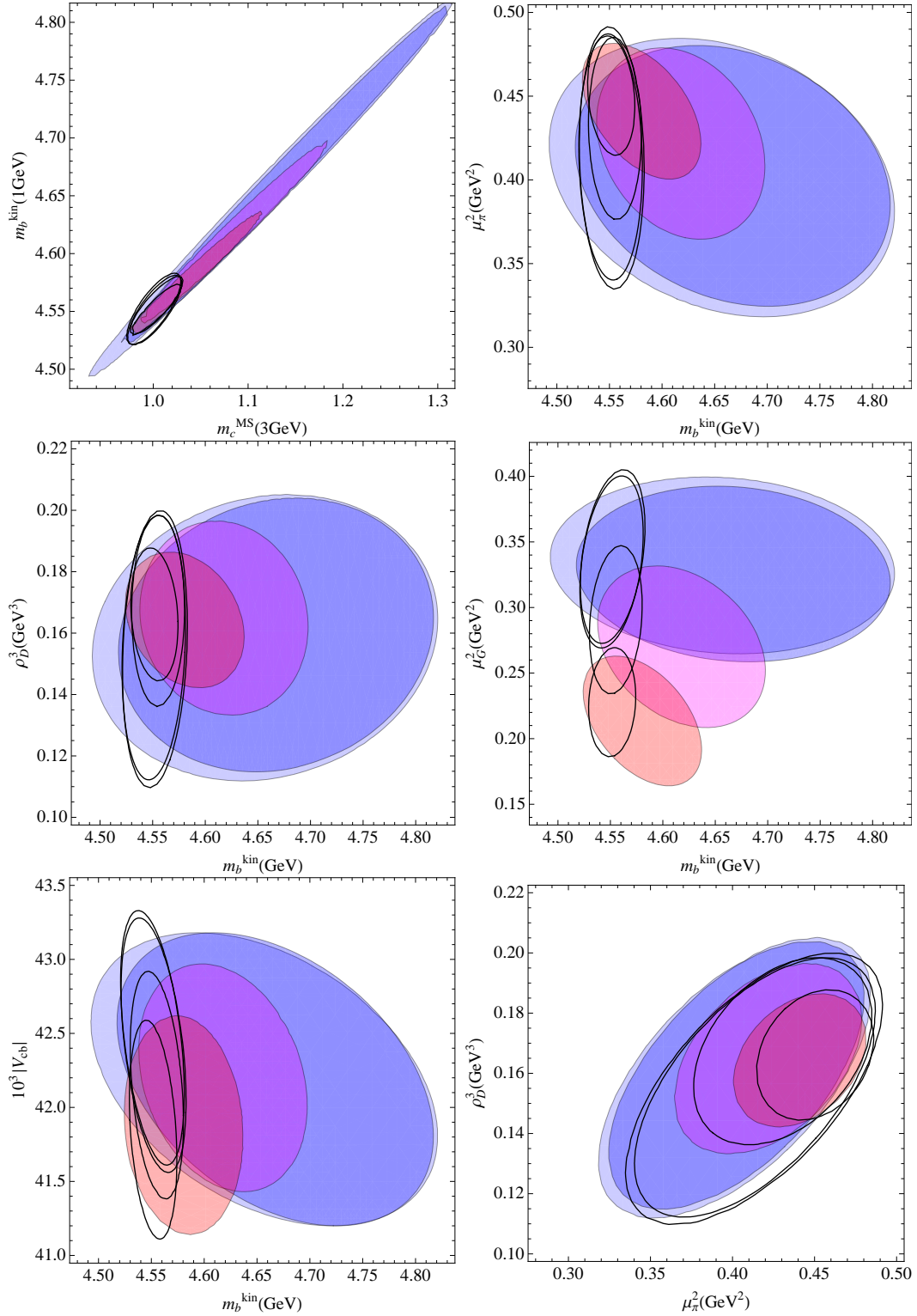


Figure 1: Two-dimensional projections of the fits performed with different assumptions for the theoretical correlations. The orange, magenta, blue, light blue 1-sigma regions correspond to scenarios A,B,C,D ( $\Delta = 0.25$  GeV), respectively. The black contours show the same regions when the  $m_c$  constraint of Ref. [13] is employed.

In general, the results depend sensitively on the option adopted. In the case of the heavy quark masses, which are strongly correlated, we observe large errors that tend to increase in going from **A** to **D**, although the central values are quite consistent. The results of the fits for the non-perturbative parameters depend even stronger on the option, in particular this is the case for  $\mu_G^2$ , which has a very low value — incompatible with (6) — in scenario **A**, and increases as correlations are relaxed.

Fig. 1 also shows that the final uncertainty on some of the parameters can be much smaller than the "safety" range we have used in the evaluation of the theory errors. Consider for instance the final error on  $\rho_D^3$ : in scenario **A** it is as low as 0.02, which is approximately 15% of the central value, much below the 30% we have employed. Evidently, the fit has found a direction in the parameter space with much lower uncertainty. On the other hand, when we relax the degree of correlation, as in options **C** and **D**, the final relative uncertainty on  $\rho_D^3$  is close to 30%. In the next Section we will study the impact of additional constraints on the heavy quark masses on these fits.

## 4 Heavy quark mass constraints

The inclusion of external precise constraints in the fit decreases the errors and may neutralize the ambiguity due to the ansatz for the theoretical correlations. It also allows us to check the consistency of the results with independent information. As semileptonic  $B$  decays alone determine precisely a linear combination of the heavy quark masses, approximately given by  $m_b - 0.8 m_c$ , see the first plot in Fig. 1, a way to maximally exploit their potential consists in including in the fit one of the recent precise  $m_c$  determinations. A review of heavy quark mass determinations is beyond the scope of this paper, see *e.g.* [3, 36]. We simply list some of the most recent ones, for the charm mass

1.  $\overline{m}_c(3 \text{ GeV}) = 0.986(13) \text{ GeV}$  [11];
2.  $\overline{m}_c(3 \text{ GeV}) = 0.986(6) \text{ GeV}$  [12];
3.  $\overline{m}_c(3 \text{ GeV}) = 0.998(29) \text{ GeV}$  [13];

and for the bottom mass

1.  $\overline{m}_b(\overline{m}_b) = 4.163(16) \text{ GeV}$  [11];
2.  $\overline{m}_b(\overline{m}_b) = 4.164(23) \text{ GeV}$  [12];
3.  $\overline{m}_b(\overline{m}_b) = 4.235(55) \text{ GeV}$  [14];
4.  $\overline{m}_b(\overline{m}_b) = 4.247(34) \text{ GeV}$  [15].

Here all the masses are expressed in the  $\overline{\text{MS}}$  scheme, and a relatively high scale, 3 GeV, is employed for the charm mass. In absolute terms, the charm mass is currently better determined than the bottom mass. This suggests to compute the moments directly in terms

$\overline{m}_c(3 \text{ GeV})$	$m_b^{kin}(1 \text{ GeV})$	$\overline{m}_b(\overline{m}_b)$
0.986(13) [11]	4.541(23)	4.171(38)
0.986(6) [12]	4.540(20)	4.170(36)
0.998(29) [13]	4.552(31)	4.182(43)

Table 2:  $b$  mass resulting from different  $m_c$  determinations. All masses are expressed in GeV.

of  $\overline{m}_c(\bar{\mu})$ , with  $2 \lesssim \bar{\mu} \lesssim 3 \text{ GeV}$ , instead of using the charm mass in the kinetic scheme. The range of  $\bar{\mu}$  is chosen to avoid large logarithms in our  $O(\alpha_s^2)$  calculation and to minimize higher orders related to the definition of  $m_c$ , which necessarily involve  $\alpha_s(\bar{\mu})$ . This  $\overline{\text{MS}}$  option for  $m_c$  is available in the code of [20] and avoids additional theoretical uncertainty due to the mass scheme conversion. In the case of the bottom mass, on the contrary, the common choice  $\overline{m}_b(\overline{m}_b)$  is not well-suited to the description of semileptonic  $B$  decays. In other words, the calculation of the moments in terms of  $\overline{m}_b(\overline{m}_b)$  would lead to large higher order corrections. While our predictions are always expressed in terms the kinetic mass  $m_b^{kin}(1 \text{ GeV})$ , the above  $m_b$  constraints can be included after converting them to the kinetic scheme. Since the relation between the kinetic and the  $\overline{\text{MS}}$  masses is known only to  $O(\alpha_s^2)$ , the ensuing uncertainty is not negligible. In Ref. [20] it has been estimated to be about 30 MeV:

$$m_b^{kin}(1 \text{ GeV}) - \overline{m}_b(\overline{m}_b) = 0.37 \pm 0.03 \text{ GeV}. \quad (8)$$

The effect of the inclusion of charm mass constraints in the semileptonic fit is illustrated in Fig. 1, where the determination of Ref. [13] is employed. As expected, the uncertainty in the  $b$  mass becomes smaller than 30 MeV in all scenarios, a marked improvement, also with respect to the precision resulting from the use of radiative moments [4]. On the other hand, there is hardly any improvement in the final precision of the non-perturbative parameters (see for instance the last plot, in the  $\mu_\pi^2$ - $\rho_D^3$  plane).

As already noted, the semileptonic moments are highly sensitive to a linear combination of the heavy quark masses. The constraints on  $m_b$  that we obtain using different  $m_c$  determinations in the fit are shown in Table 2, where we have only considered option **D** with  $\Delta = 0.25 \text{ GeV}$ . It is interesting to compare the results in the last column with the  $\overline{m}_b(\overline{m}_b)$  determinations we have listed above. The bottom mass obtained using  $m_c$  given by the Karlsruhe group [11] is perfectly consistent with their own  $m_b$  result, but also compatible with those of Refs. [12, 14]. In general, lower values of  $m_b$  are preferred. The results depend little on the scenario chosen for the theory correlations: if we choose  $\Delta = 0.2 \text{ GeV}$   $m_b$  gets lowered by 1 MeV in the first two rows, and by 2 MeV in the third. Very similar results are found using alternative scenarios for the theory correlations. Of course, one can also include in the fit both  $m_c$  and  $m_b$  determinations, but because of the scheme translation error in  $m_b$  the gain in accuracy will be limited.

When no external constraint is imposed on  $m_{c,b}$ , the semileptonic moments determine best a linear combination of the heavy quark masses which is very close to their difference.

th. corr. scenario	$m_b^{kin}$	$m_c$	$\mu_\pi^2$	$\rho_D^3$	$\mu_G^2$	$\rho_{LS}^3$	$\text{BR}_{cl\nu}(\%)$	$10^3  V_{cb} $
<b>D</b> [11]	4.541	0.987	0.414	0.154	0.340	-0.147	10.65	42.42
$\bar{m}_c(3\text{GeV})$	0.023	0.013	0.078	0.045	0.066	0.098	0.16	0.86
<b>A</b> [11]	4.540	0.987	0.454	0.167	0.234	-0.078	10.45	41.85
$\bar{m}_c(3\text{GeV})$	0.014	0.013	0.035	0.022	0.040	0.085	0.13	0.74
<b>B</b> [11]	4.542	0.987	0.457	0.184	0.290	-0.135	10.51	42.15
$\bar{m}_c(3\text{GeV})$	0.017	0.013	0.056	0.035	0.056	0.095	0.14	0.77
<b>C</b> [11]	4.539	0.987	0.415	0.155	0.336	-0.147	10.65	42.45
$\bar{m}_c(3\text{GeV})$	0.022	0.013	0.073	0.043	0.066	0.098	0.16	0.86
<b>D</b> [11]	4.538	0.986	0.415	0.153	0.336	-0.145	10.65	42.46
$\bar{m}_c(3\text{GeV}), m_b$	0.018	0.012	0.078	0.045	0.064	0.098	0.16	0.84
<b>D</b> [13]	4.552	1.001	0.413	0.155	0.339	-0.146	10.65	42.39
$\bar{m}_c(3\text{GeV})$	0.031	0.029	0.078	0.045	0.066	0.098	0.16	0.86
<b>D</b> [11]	4.548	1.092	0.428	0.158	0.344	-0.146	10.66	42.24
$m_c^{kin}$	0.023	0.020	0.079	0.045	0.066	0.098	0.16	0.85
<b>D</b> [11]	4.553	1.088	0.428	0.155	0.328	-0.139	10.67	42.42
$\bar{m}_c(2\text{GeV}), m_b$	0.018	0.013	0.079	0.045	0.064	0.098	0.16	0.83

Table 3: Global fits with  $m_c$  constraints. Scenario **D** has  $\Delta = 0.25$  GeV. All parameters except  $m_c$  are in the kinetic scheme with cutoff at 1 GeV. The definition of  $m_c$  and the use of an  $m_b$  constraint are marked in the first column, directly under the reference for their constraints.

Using scenario **D** with  $\Delta = 0.25$  GeV we obtain

$$m_b^{kin}(1\text{ GeV}) - 0.85 \bar{m}_c(3\text{ GeV}) = 3.701 \pm 0.019\text{ GeV}, \quad (9)$$

and similar results with the other scenarios (the error is as low as 12 MeV in scenario **A**). The ratio of the two masses is  $\bar{m}_c(3\text{ GeV})/m_b^{kin}(1\text{ GeV}) = 0.2172(25)$ . In the case the kinetic scheme is also adopted for  $m_c$ , the linear combination is slightly different and Eq. (9) becomes

$$m_b^{kin}(1\text{ GeV}) - 0.7 m_c^{kin}(1\text{ GeV}) = 3.784 \pm 0.019\text{ GeV}. \quad (10)$$

The results of a few fits are reported in Table 3. We choose the first one as our *default* fit. All the fits include a constraint on  $m_c$ , from either Ref. [11] or [13], and two fits both mass constraints from Ref. [11]. In the latter case we have used (8) to translate  $\bar{m}_b(\bar{m}_b) = 4.163(16)$  GeV into  $m_b^{kin} = 4.533(32)$  GeV (the  $\alpha_s$  dependence of Eq. (8) partly compensates that of  $\bar{m}_b(\bar{m}_b)$ ). The fits are generally good, ranging from  $\chi^2/d.o.f. = 0.32$  for the default fit, to 0.95 for case **B** and 1.18 for case **A**. The value of  $|V_{cb}|$  is computed using

$$|V_{cb}| = \sqrt{\frac{|V_{cb}|^2 \text{BR}_{cl\nu}}{\tau_B \Gamma_{B \rightarrow X_c \ell \nu}^{OPE}}}, \quad (11)$$

with  $\tau_B = 1.582(7)$  ps. Its theoretical error is computed combining in quadrature the parametric uncertainty that results from the fit, and an additional 1.4% theoretical error to

$m_b^{kin}$	$\overline{m}_c(3 \text{ GeV})$	$\mu_\pi^2$	$\rho_D^3$	$\mu_G^2$	$\rho_{LS}^3$	$\text{BR}_{cl\nu}$	$ V_{cb} $
1	0.476	-0.101	0.218	0.484	-0.158	-0.092	-0.443
	1	-0.013	0.009	-0.014	0.004	0.012	-0.014
		1	0.613	0.007	0.056	0.126	0.342
			1	-0.041	-0.126	0.048	0.179
				1	-0.013	-0.023	-0.164
					1	-0.007	0.009
						1	0.461
							1

Table 4: Correlation matrix for the default fit: scenario **D**,  $\Delta = 0.25 \text{ GeV}$ ,  $m_c$  from [11].

$m_b^{kin}$	$\overline{m}_c(3 \text{ GeV})$	$\mu_\pi^2$	$\rho_D^3$	$\mu_G^2$	$\rho_{LS}^3$	$\text{BR}_{cl\nu}$	$ V_{cb} $
1	0.405	-0.082	0.180	0.412	-0.130	-0.075	-0.389
	1	0.003	-0.027	-0.098	0.030	0.028	0.041
		1	0.626	0.025	0.051	0.123	0.338
			1	-0.080	-0.116	0.055	0.207
				1	0.013	-0.008	-0.120
					1	-0.012	-0.007
						1	0.463
							1

Table 5: Correlation matrix for the fit with both  $m_c$  and  $m_b$  from [11], scenario **D**,  $\Delta = 0.25 \text{ GeV}$ .

take into account missing higher order corrections in the expression for the semileptonic width [20, 37]. An approximate formula for  $|V_{cb}|$  using the above  $\tau_B$  value and  $m_c(3 \text{ GeV})$  is

$$|V_{cb}| = 0.042316 \left[ 1 + 0.54 (\alpha_s - 0.219) - 0.653 (m_b^{kin} - 4.55) + 0.489 (\overline{m}_c(3 \text{ GeV}) - 1) \right. \\ \left. + 0.016 (\mu_\pi^2 - 0.44) + 0.058 (\mu_G^2 - 0.32) + 0.12 (\rho_D^3 - 0.2) - 0.013 (\rho_{LS}^3 + 0.15) \right], (12)$$

where all dimensionfull quantities are expressed in GeV.

A few comments are now in order:

- i)* The inclusion of the  $m_c$  constraint has stabilized the fits with respect to the ansatz for the theory correlations. The only exception is represented by scenario **A**, which mostly deviates in the values of  $\mu_\pi^2$  and  $\mu_G^2$  and in the magnitude of the uncertainties. In any case, because of the above discussion, this scenario should be abandoned.
- ii)* The low  $\chi^2$  of the default fit is due to the large theoretical uncertainties we have assumed. It may be tempting to interpret it as evidence that the theoretical errors have been overestimated. However, higher order corrections may effectively shift the

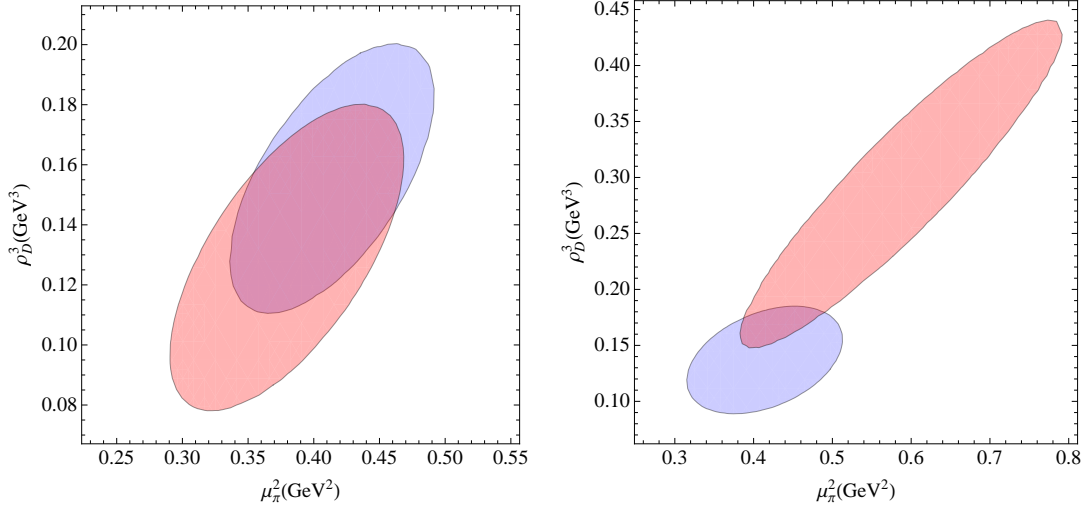


Figure 2:  $1\sigma$  projections on the  $\mu_\pi^2, \rho_D^3$  plane of the default fit. Left: with (blue) and without (red) moments measured at  $E_{\text{cut}} > 1.2 \text{ GeV}$ ; right: with only hadronic moments (blue) and only leptonic moments (red).

parameters of the  $O(1/m_b^2)$  and  $O(1/m_b^3)$  contributions. If we want to maintain the formal definition of these parameters, and to be able to use them elsewhere, we therefore have to take into account the potential shift they may experience because of higher order effects.

- iii) The third hadronic moment by Delphi was neglected in previous analyses in the kinetic scheme. Its main effect on our default fit is to decrease  $\rho_D^3$  by about 10% and  $\mu_\pi^2$  by about 3%.
- iv) The fits with a constraint on  $m_c$  are quite stable with respect to a change of inputs. In particular, we have found small differences when experimental data at high  $E_{\text{cut}}$  are excluded, and when only hadronic or leptonic moments are considered. While the results for the heavy quark masses do not change appreciably, the results for the OPE parameters change within errors. We show in Fig. 2 the projection onto the  $\mu_\pi^2 - \rho_D^3$  plane of the default fit with/without moments at  $E_{\text{cut}} > 1.2 \text{ GeV}$  and with only leptonic and only hadronic moments.
- v) One may wonder whether the inclusion of moments measured at different values of  $E_{\text{cut}}$  really benefits the final accuracy. We have run our default fit with only one  $E_{\text{cut}}$  for each moment per experiment and found slightly larger errors (26 MeV on  $m_b$  and  $0.1 \text{ GeV}^2$  on  $\mu_\pi^2$ ) than when we use the full set of data. The benefit is therefore minor but non-negligible. Of course, the inclusion of moments at different cuts plays a much more important role in scenarios **A** and **B**.
- vi) In the kinetic scheme the inequalities  $\mu_\pi^2(\mu) \geq \mu_G^2(\mu)$ ,  $\rho_D^3(\mu) \geq -\rho_{LS}^3(\mu)$  hold at arbitrary

values of the cutoff  $\mu$ . The central values of the fits always satisfy the inequalities.

- vii) The value of  $|V_{cb}|$  is generally larger than in previous analyses. This is mostly due to the higher  $\text{BR}_{c\ell\nu}$ , as can be seen in Table 3. Indeed, the low value of  $\text{BR}_{c\ell\nu}$  is the most distinctive feature of scenario **A** and **B**, and the most relevant for the  $|V_{cb}|$  determination. It is worth noting that the latest CKM global fit [1] gives  $|V_{cb}| = 0.04273(77)$ , with a marked preference for a high value of  $|V_{cb}|$ .
- viii) The  $O(\alpha_s^2)$  perturbative expansion for the  $b \rightarrow c\ell\nu$  width has relative large coefficients when  $\bar{m}_c(3 \text{ GeV})$  is employed, while the situation improves in case one uses  $\bar{m}_c(2 \text{ GeV})$  or  $m_c^{\text{kin}}(1 \text{ GeV})$ , see the Appendix of [20]. We have briefly studied what happens with  $\bar{m}_c(2 \text{ GeV})$ : the answer depends little on the way one computes it from  $\bar{m}_c(3 \text{ GeV}) = 0.986(13) \text{ GeV}$ . Using three loop RGE evolution leads to  $\bar{m}_c(2 \text{ GeV}) = 1.091(14) \text{ GeV}$ , and in scenario **D** one gets the results in the last row of Table 3, with  $|V_{cb}|$  very close to the other fits. Table 3 also reports results for a fit to the charm mass expressed in the kinetic scheme. In this case we employ scenario **D** as in the default fit, and use a constraint on  $m_c^{\text{kin}}(1 \text{ GeV})$  derived from the  $\bar{m}_c(3 \text{ GeV})$  determination of [11]. Using the translation formula given in [20] we obtain  $m_c^{\text{kin}}(1 \text{ GeV}) = 1.091 \pm 0.020 \text{ GeV}$ . The value of the BR and of  $|V_{cb}|$  are consistent with the results of the  $\overline{\text{MS}}$  scheme fits.

Because of strong correlations, the measurements listed in Table 1 are only a subset of all the measured moments. In order to gain a visual appreciation of the quality of the default fit and to see how well it agrees also with the measurements that are not included, we show in Figs. 3 and 4 the leptonic and hadronic moments measurements compared with their theoretical prediction with theory uncertainty.

## 5 Implications of the default fit

### 5.1 Semileptonic phase space ratio

It is particularly convenient to normalize the branching fraction of the rare decays  $B \rightarrow X_s \gamma$  and  $B \rightarrow X_s \ell^+ \ell^-$  to the semileptonic one,  $\text{BR}_{c\ell\nu}$ . In this context the semileptonic phase space ratio

$$C = \left| \frac{V_{ub}}{V_{cb}} \right|^2 \frac{\Gamma[\bar{B} \rightarrow X_c e \bar{\nu}]}{\Gamma[\bar{B} \rightarrow X_u e \bar{\nu}]} \quad (13)$$

is usually factorized [38–41].  $C$  can be calculated using the OPE and the results of the fit to the semileptonic moments. In principle, the  $B \rightarrow X_u \ell \bar{\nu}$  width is also sensitive to Weak Annihilation (WA) contributions, see e.g. [41], which are poorly known but cancel out in the rare decay width. As far as the normalization of rare decays is concerned, WA effects can therefore be ignored. Even neglecting WA, however, the value of  $C$  does depend on the scale at which the WA matrix element is assumed to vanish. In the following we follow [41] and use  $\mu_{WA} = m_b/2$ .

In Ref. [41]  $C$  was computed in the kinetic scheme, based on the fits performed by HFAG at that time. The result was  $C = 0.546 \pm 0.016(\text{pert}) \pm 0.017(\text{HQE})$ , where the first

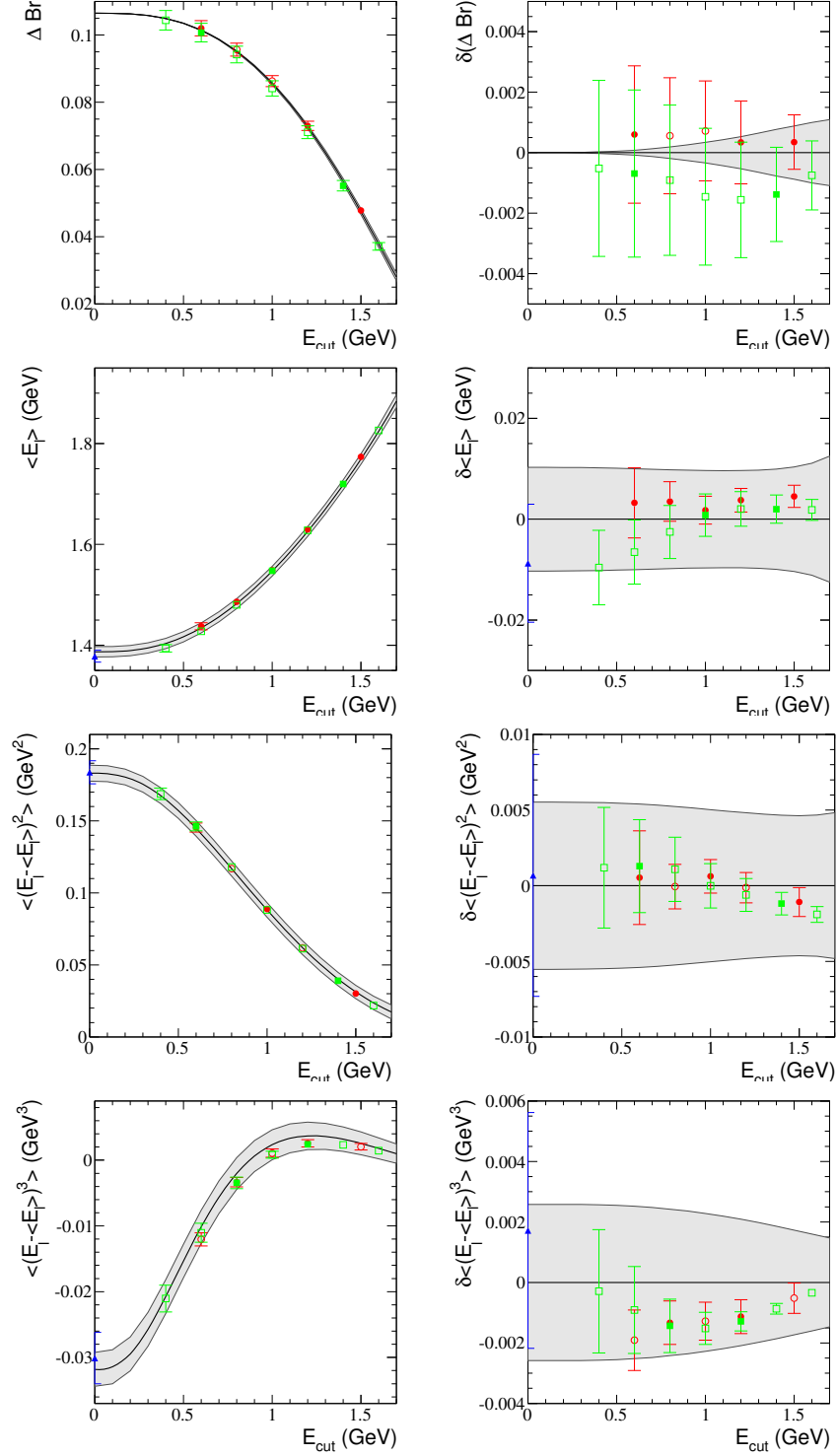


Figure 3: Default fit predictions for  $R^*, \ell_{1,2,3}$  compared with measured values in absolute terms (left) and as deviations ( $\delta$ , right) from the predictions as a function of  $E_{cut}$ . In all plots, the grey band is the theory prediction with total theory error. BaBar data are shown by circles, Belle by squares and other experiments (DELPHI, CDF, CLEO) by triangles. Filled symbols mean that the point was used in the fit. Open symbols are measurements that were not used in the fit.

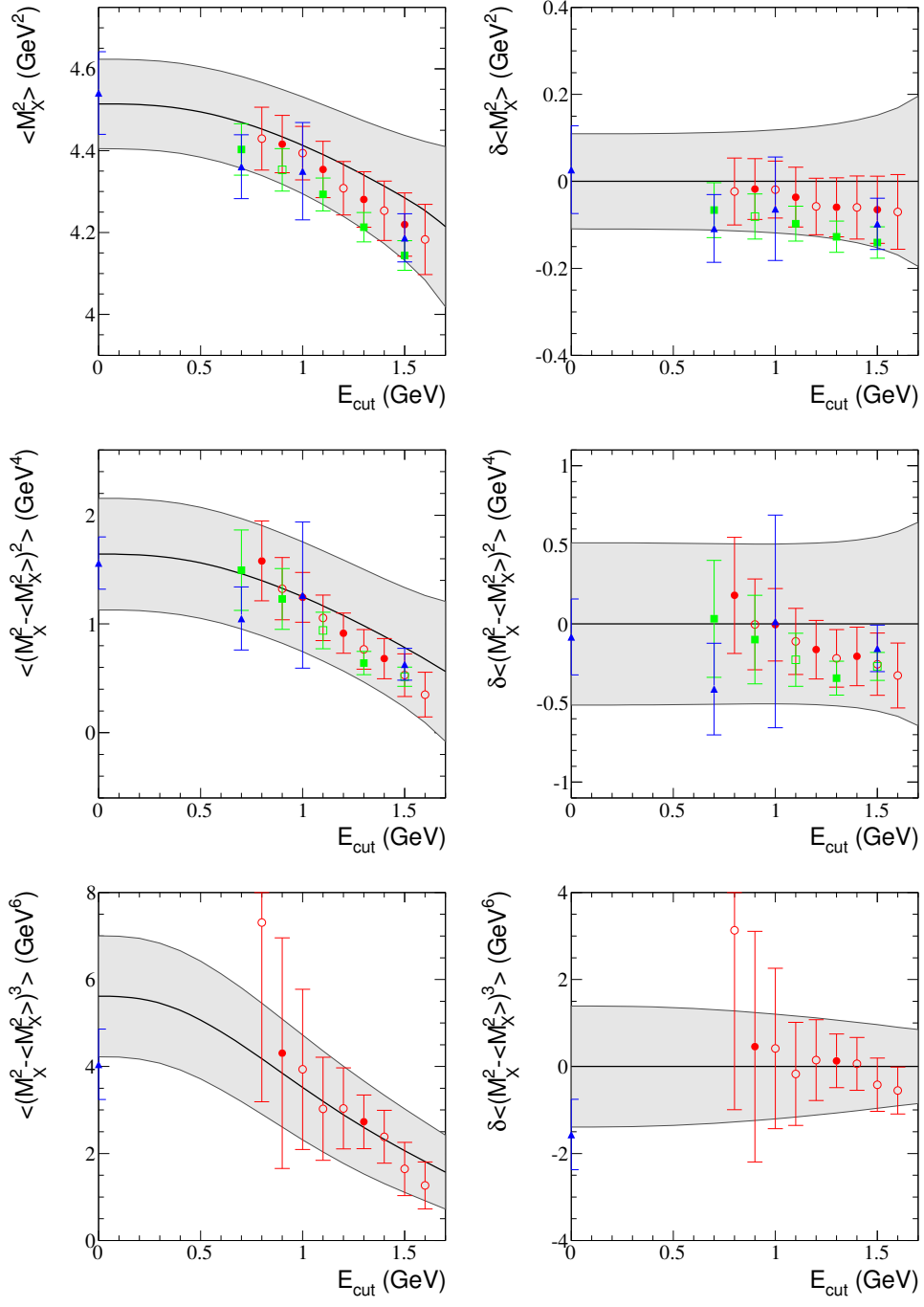


Figure 4: Same as in Fig. 3 for  $h_{1,2,3}$ .

uncertainty refers to higher order perturbative contributions, and the second is associated with the semileptonic fit. A different result,  $C = 0.582 \pm 0.016$ , was reported in [8] in the 1S scheme, see also the first paper of [40] for additional details. The central value has already been converted to our convention with  $\mu_{WA} = m_b/2$ . The mild discrepancy between these two values was partly related to the way the fit was performed in the kinetic scheme. Now it has considerably reduced, as we will see in a moment.

In order to compute  $C$  with our default fit we need to adapt the calculation of [41] to the use of a charm mass in the  $\overline{\text{MS}}$  scheme at  $\mu = 2$  or  $3 \text{ GeV}$ . Here we give the two corresponding approximate formulas,

$$C = g(\rho) \left\{ 0.903 - 0.595 \delta_{\alpha_s} + 0.0405 \delta_b - 0.1137 (\overline{m}_c(2 \text{ GeV}) - 1.05 \text{ GeV}) \right. \\ \left. - 0.0184 \mu_G^2 - 0.199 \rho_D^3 + 0.004 \rho_{LS}^3 \right\}, \quad (14)$$

$$C = g(\rho) \left\{ 0.849 - 0.92 \delta_{\alpha_s} + 0.0596 \delta_b - 0.2237 (\overline{m}_c(3 \text{ GeV}) - 1 \text{ GeV}) \right. \\ \left. - 0.0167 \mu_G^2 - 0.203 \rho_D^3 + 0.004 \rho_{LS}^3 \right\}, \quad (15)$$

where  $g(\rho) = 1 - 8\rho + 8\rho^3 - \rho^4 - 12\rho^2 \ln \rho$ ,  $\rho = (m_c/m_b)^2$ ,  $\delta_{\alpha_s} = \alpha_s(4.6 \text{ GeV}) - 0.22$ , and  $\delta_b = m_b - 4.55 \text{ GeV}$ . The approximate formulas reproduce the complete calculation to better than 0.4% in the range  $4.45 < m_b < 4.65 \text{ GeV}$ ,  $0.9 < \overline{m}_c(3 \text{ GeV}) < 1.1 \text{ GeV}$ ,  $0.95 < \overline{m}_c(2 \text{ GeV}) < 1.15 \text{ GeV}$ . Using our default fit we obtain

$$C = 0.574 \pm 0.008, \quad (16)$$

with an additional  $\sim 3\%$  theoretical error. The result is identical if we include  $m_b$  from [11] in the fit. In scenario **B** with both  $m_{c,b}$  from [11] we get  $C = 0.572(8)$ . In comparison with [41], the parametric uncertainty has reduced by a factor 2, mostly thanks to the new charm mass constraint, and the central value has increased by about  $1\sigma$ . Our result is in good agreement with that of [8].

One may worry that the perturbative series of  $C$  in terms of  $\overline{m}_c(3 \text{ GeV})$  has relatively large coefficients, as witnessed by the strong  $\alpha_s$  dependence in (15), and that it likely involves large  $O(\alpha_s^3)$  terms. In this respect, the situation is somewhat better if one employs the kinetic charm mass or  $\overline{m}_c(2 \text{ GeV})$ , see (14). Evolving  $\overline{m}_c(3 \text{ GeV}) = 0.986(13) \text{ GeV}$  [11] down to  $2 \text{ GeV}$ , and using  $\overline{m}_c(2 \text{ GeV}) = 1.091(14) \text{ GeV}$  and  $m_b^{\text{kin}} = 4.533(32) \text{ GeV}$  as constraints in a fit to  $\overline{m}_c(2 \text{ GeV})$  we get

$$C = 0.566 \pm 0.008, \quad (17)$$

again with additional 3% theoretical uncertainty. This is compatible with the result in Eq. (16), and might be preferred as a reference value.

Of course, the factor  $C$  is just one component of the calculation of rare  $B$  decays. What actually enters inclusive  $B$  decays is  $\text{BR}_{c\ell\nu}/C$ , and there are additional power-suppressed corrections that affect the width and depend on the same parameters that determine  $C$ , as well as charm loops in the perturbative corrections. As precision increases, it is no longer obvious that the factorization of  $C$  is still advantageous, except as a bookkeeping device.

Nevertheless, the results of our fit, with the complete correlation matrix, are all one needs for a careful analysis of the parametric uncertainty in those cases.

Finally, it is worth reminding that, in the case of  $B \rightarrow X_s \gamma$ , it is often necessary to extrapolate measurements performed with a cut on the photon energy higher than about 1.6 GeV to lower photon energies, where the local OPE is expected to work better. This extrapolation can be performed using different techniques [42], but it crucially depends on precise HQE parameters, namely on the results of semileptonic fits.

## 5.2 Local contributions to the zero-recoil sum rule

The  $B \rightarrow D^* \ell \nu$  form factor at zero recoil can be estimated using heavy quark sum rules [6, 43]. The form-factor  $\mathcal{F}(1)$  is obtained by separating the elastic  $B \rightarrow D^*$  transition contribution from the total inelastic transition at zero-recoil:

$$I_0(\varepsilon_M) = \mathcal{F}^2(1) + I_{\text{inel}}(\varepsilon_M), \quad (18)$$

where  $I_{\text{inel}}(\varepsilon_M)$  is related to the sum of the differential decay probabilities into the excited states with mass up to  $M_{D^*} + \varepsilon_M$  in the zero recoil kinematics.

The OPE allows us to calculate the amplitude  $I_0(\varepsilon_M)$  in the short-distance expansion provided  $|\varepsilon|$  is sufficiently large compared to the ordinary hadronic mass scale. Setting  $\varepsilon = \mu^{\text{kin}}$

$$I_0(\mu^{\text{kin}}) = \xi_A^{\text{pert}}(\mu^{\text{kin}}) - \Delta_{1/m^2} - \Delta_{1/m^3} + \dots, \quad (19)$$

where the ellipses stand for higher order contributions and  $\xi_A^{\text{pert}}$  represents a perturbative contribution. The latter was computed in Ref. [6] to  $O(\alpha_s^2)$ :  $\sqrt{\xi_A^{\text{pert}}}(0.75 \text{ GeV}) = 0.98 \pm 0.01$ . The leading power contributions to  $I_0$  were calculated in Refs. [43] to order  $1/m_Q^2$  and in Ref. [44] to order  $1/m_Q^3$  and read

$$\begin{aligned} \Delta_{1/m^2} &= \frac{\mu_G^2}{3m_c^2} + \frac{\mu_\pi^2 - \mu_G^2}{4} \left( \frac{1}{m_c^2} + \frac{2}{3m_c m_b} + \frac{1}{m_b^2} \right), \\ \Delta_{1/m^3} &= \frac{\rho_D^3 - \frac{1}{3}\rho_{LS}^3}{4m_c^3} + \frac{1}{12m_b} \left( \frac{1}{m_c^2} + \frac{1}{m_c m_b} + \frac{3}{m_b^2} \right) (\rho_D^3 + \rho_{LS}^3). \end{aligned}$$

In the kinetic scheme the nonperturbative parameters  $\mu_\pi^2$ ,  $\mu_G^2$ ,  $\rho_D^3$  and  $\rho_{LS}^3$  all depend on the hard Wilsonian cutoff  $\mu^{\text{kin}}$ . Since the heavy quark expansion of  $I_0$  involves inverse powers of  $m_c$ , the cutoff must satisfy  $\mu^{\text{kin}} \ll 2m_c$  and it is better to have it lower than 1 GeV. We therefore take the values of the OPE parameters extracted from our default fit with  $m_c$  in the kinetic scheme, evolve them down to  $\mu^{\text{kin}} = 0.75 \text{ GeV}$  and find

$$\Delta_{1/m^2} = 0.084 \pm 0.017, \quad \Delta_{1/m^3} = 0.021 \pm 0.008, \quad (20)$$

and for the sum

$$\Delta_{1/m^2} + \Delta_{1/m^3} = 0.104 \pm 0.023. \quad (21)$$

If we use scenario **B** we get a slightly larger value  $0.111 \pm 0.016$ , closer to the preliminary result  $0.118 \pm 0.015$  given in [6] and obtained using that scenario. The quantity in (21) is an important ingredient of the heavy quark sum rule estimate of  $\mathcal{F}(1)$ : the present update does not affect significantly the results of [6].

### 5.3 Impact on inclusive $|V_{ub}|$ determination

In order to get a rough estimate of the precision that can be reached applying the results of our default fit to the semileptonic  $B \rightarrow X_u \ell \nu$  analyses, we use the information given in the kinetic scheme analysis of Ref. [45]. Recent experimental studies have considered lower cutoffs on the lepton momentum as low as 1 GeV, which is very close to the total decay width and for which a local OPE description is perfectly adequate. Therefore, we take Eq. (45) of Ref. [45] and compute the parametric uncertainty on the total  $B \rightarrow X_u \ell \nu$  width using the results of the default fit. We obtain a 2.2% error that translates into a 1.1% parametric uncertainty on  $|V_{ub}|$ . A slightly smaller uncertainty, 1.8%, is obtained if one employs a fit that also includes the constraint on  $m_b$  from [11]. Since the uncertainty is dominated by that of  $m_b$ , better determinations of this mass will result in further reduction of the parametric error.

In summary, the parametric uncertainty on the total  $B \rightarrow X_u \ell \nu$  width is about 2% and can be reduced in the future; it will have to be considered together with a  $\gtrsim 1\%$  theoretical uncertainty. As mentioned above this should essentially hold even for a lower cut on the lepton momentum around 1 GeV is applied. On the other hand, for higher cuts the local OPE is no longer sufficient and the sensitivity to  $m_b$  gets stronger: these analyses will benefit of a better determination of  $m_b$  even more.

## 6 Summary

In this paper we have reassessed the whole strategy of global fits to the semileptonic moments. We have shown that the results depend sensitively not only on the estimate of the theoretical uncertainties, but also on the assumptions about their correlation. We have studied the impact of precise determinations of the heavy quark masses from independent data on the global fits and shown that their use leads to more precise results, which depend less on the assumptions on the theoretical correlations. Using a determination of  $m_c$  with 13 MeV uncertainty we were able to determine  $m_b$  within about 20 MeV, in good agreement and competitive with some of the most precise  $m_b$  determinations. In the absence of external constraints on the heavy quark masses, the semileptonic moments determine their difference with a 20 MeV uncertainty, see Eq. (9). This is a robust NNLO relation that we find stable against theoretical assumptions.

The value of  $|V_{cb}|$  that we obtain is higher than in previous analyses, but compatible with the prediction of a global CKM fit in the Standard Model [1]; it has a total 2% accuracy, which is dominated by theoretical errors. We have also studied the impact on the new fits on the calculation of the semileptonic phase space ratio  $C$ , on the power corrections to the

zero-recoil sum rule, and on the extraction of  $|V_{ub}|$ .

Theoretical uncertainties are the major obstacle to an accurate determination of  $|V_{cb}|$  using inclusive semileptonic  $B$  decays. Our theoretical errors are essentially determined by a conservative estimate of the dominant sources of higher order corrections. There are therefore good prospects for improvement, related to the completion of the calculation of  $O(\alpha_s \mu_G^2/m_b^2)$  and to the inclusion of the  $O(1/m_Q^{4,5})$  corrections. A more significant reduction of the error on  $|V_{cb}|$  will also require a calculation of perturbative corrections to the coefficient of the Darwin operator. In contrast, the experimental situation is much better at the moment and will further improve at Belle-II.

## Acknowledgements

PG is grateful to Lorenzo Magnea and to the late Kolya Uraltsev for useful discussions, and to Mikolaj Misiak and Matthias Steinhauser for carefully reading a preliminary version of this paper. This work is supported in part by MIUR under contract 2010YJ2NYW\_006.

## References

- [1] UTFit Collaboration, M. Bona *et al.*, JHEP **10**, 081 (2006), hep-ph/0606167, and <http://utfit.org> for the Winter 2013 update. See also CKMfitter Collaboration, <http://ckmfitter.in2p3.fr>.
- [2] I. Bigi, N. Uraltsev and A. Vainshtein, *Phys. Lett.* **B293** (1992) 430 and *Phys. Rev. Lett.* **71** (1993) 496; B. Blok, L. Koyrakh, M. Shifman and A. Vainshtein, *Phys. Rev.* **D49** (1994) 3356; A. V. Manohar and M. B. Wise, *Phys. Rev. D* **49** (1994) 1310.
- [3] M. Antonelli, D. M. Asner, D. A. Bauer, T. G. Becher, M. Beneke, A. J. Bevan, M. Blanke and C. Bloise *et al.*, *Phys. Rept.* **494** (2010) 197 [arXiv:0907.5386 [hep-ph]].
- [4] Heavy Flavour Averaging Group (HFAG), Y. Amhis *et al.*, arXiv:1207.1158 [hep-ex], <http://www.slac.stanford.edu/xorg/hfag/> .
- [5] J. A. Bailey *et al.* [Fermilab Lattice and MILC Collaborations], PoS LATTICE **2010** (2010) 311 [arXiv:1011.2166 [hep-lat]].
- [6] P. Gambino, T. Mannel and N. Uraltsev, JHEP **1210** (2012) 169 [arXiv:1206.2296 [hep-ph]] and *Phys. Rev. D* **81** (2010) 113002 [arXiv:1004.2859 [hep-ph]].
- [7] B. Aubert *et al.* [BABAR Coll.], *Phys. Rev. Lett.* **93** (2004) 011803 [hep-ex/0404017].
- [8] C. W. Bauer *et al.*, *Phys. Rev. D* **70** (2004) 094017 [hep-ph/0408002] v3.
- [9] O. Buchmuller, H. Flacher, *Phys. Rev.* **D73** (2006) 073008 [hep-ph/0507253].
- [10] P. Gambino and C. Schwanda, arXiv:1102.0210 [hep-ex].

- [11] K. G. Chetyrkin, J. H. Kuhn, A. Maier, P. Maierhofer, P. Marquard, M. Steinhauser and C. Sturm, *Phys. Rev. D* **80** (2009) 074010 [arXiv:0907.2110 [hep-ph]].
- [12] I. Allison *et al.* [HPQCD Collaboration], *Phys. Rev.* **D78**, 054513 (2008) [arXiv:0805.2999 [hep-lat]]; C. McNeile *et al.* [HPQCD Collaboration], *Phys. Rev. D* **82** (2010) 034512 [arXiv:1004.4285 [hep-lat]].
- [13] B. Dehnadi, A. H. Hoang, V. Mateu and S. M. Zebarjad, arXiv:1102.2264 [hep-ph]; AIP Conf. Proc. **1441** (2012) 628.
- [14] A. Hoang, P. Ruiz-Femenia and M. Stahlhofen, *JHEP* **1210** (2012) 188 [arXiv:1209.0450 [hep-ph]].
- [15] W. Lucha, D. Melikhov and S. Simula, arXiv:1305.7099 [hep-ph].
- [16] G. Paz, arXiv:1011.4953 [hep-ph].
- [17] A. Pak and A. Czarnecki, *Phys. Rev. Lett.* **100** (2008) 241807 [arXiv:0803.0960 [hep-ph]].
- [18] K. Melnikov, *Phys. Lett. B* **666** (2008) 336 [arXiv:0803.0951 [hep-ph]].
- [19] S. Biswas and K. Melnikov, *JHEP* **1002** (2010) 089 [arXiv:0911.4142 [hep-ph]].
- [20] P. Gambino, *JHEP* **1109** (2011) 055 [arXiv:1107.3100 [hep-ph]].
- [21] P. Gambino and N. Uraltsev, *Eur. Phys. J. C* **34** (2004) 181 [arXiv:hep-ph/0401063].
- [22] T. Becher, H. Boos and E. Lunghi, *JHEP* **0712** (2007) 062 [arXiv:0708.0855 [hep-ph]].
- [23] A. Alberti, T. Ewerth, P. Gambino and S. Nandi, *Nucl. Phys. B* **870** (2013) 16 [arXiv:1212.5082 [hep-ph]].
- [24] T. Mannel, S. Turczyk and N. Uraltsev, *JHEP* **1011** (2010) 109 [arXiv:1009.4622 [hep-ph]].
- [25] M. Grell and A. Kapustin, *Phys. Rev.* **D55** (1997) 6924.
- [26] B. Aubert *et al.* [BABAR Collaboration], *Phys. Rev. D* **81**, 032003 (2010) [arXiv:0908.0415 [hep-ex]].
- [27] B. Aubert *et al.* [BABAR Collaboration], *Phys. Rev. D* **69**, 111104 (2004) [arXiv:hep-ex/0403030].
- [28] P. Urquijo *et al.*, *Phys. Rev. D* **75**, 032001 (2007) [arXiv:hep-ex/0610012].
- [29] C. Schwanda *et al.* [BELLE Collaboration], *Phys. Rev. D* **75**, 032005 (2007) [arXiv:hep-ex/0611044].

- [30] C. Schwanda *et al.* [Belle Collaboration], Phys. Rev. D **78**, 032016 (2008) [arXiv:0803.2158 [hep-ex]].
- [31] D. E. Acosta *et al.* [CDF Collaboration], Phys. Rev. D **71**, 051103 (2005) [arXiv:hep-ex/0502003].
- [32] S. E. Csorna *et al.* [CLEO Collaboration], Phys. Rev. D **70**, 032002 (2004) [arXiv:hep-ex/0403052].
- [33] J. Abdallah *et al.* [DELPHI Collaboration], Eur. Phys. J. C **45**, 35 (2006) [arXiv:hep-ex/0510024].
- [34] I. I. Y. Bigi, M. A. Shifman, N. Uraltsev and A. I. Vainshtein, Phys. Rev. D **56** (1997) 4017 [arXiv:hep-ph/9704245] and Phys. Rev. D **52** (1995) 196 [arXiv:hep-ph/9405410].
- [35] N. Uraltsev, Phys. Lett. B **545** (2002) 337 [hep-ph/0111166].
- [36] J. Beringer *et al.* (Particle Data Group), Phys. Rev. D **86** (2012) 010001.
- [37] D. Benson, I. I. Bigi, T. Mannel and N. Uraltsev, Nucl. Phys. B **665** (2003) 367 [arXiv:hep-ph/0302262].
- [38] P. Gambino and M. Misiak, Nucl. Phys. B **611** (2001) 338 [hep-ph/0104034].
- [39] C. Bobeth, P. Gambino, M. Gorbahn and U. Haisch, JHEP **0404** (2004) 071 [hep-ph/0312090].
- [40] M. Misiak and M. Steinhauser, Nucl. Phys. B **764** (2007) 62 [arXiv:hep-ph/0609241]; M. Misiak *et al.*, Phys. Rev. Lett. **98** (2007) 022002 [arXiv:hep-ph/0609232].
- [41] P. Gambino and P. Giordano, Phys. Lett. B **669** (2008) 69 [arXiv:0805.0271 [hep-ph]].
- [42] D. Benson, I. I. Bigi and N. Uraltsev, Nucl. Phys. B **710** (2005) 371 [hep-ph/0410080]; M. Neubert, Eur. Phys. J. C **40** (2005) 165 [hep-ph/0408179].
- [43] I.I. Bigi, M. Shifman, N. Uraltsev and A. Vainshtein, Phys. Rev. D **52** (1995) 196; M.A. Shifman, N.G. Uraltsev and A.I. Vainshtein, Phys. Rev. D **51** (1995) 2217.
- [44] I. Bigi, M Shifman, N.G. Uraltsev, *Ann. Rev. Nucl. Part. Sci.* **47** (1997) 591.
- [45] P. Gambino, P. Giordano, G. Ossola and N. Uraltsev, JHEP **0710** (2007) 058 [arXiv:0707.2493 [hep-ph]].